IEEE Access
Multidisciplinary | Rapid Review | Open Access Journal

Received August 3, 2021, accepted August 12, 2021, date of publication August 24, 2021, date of current version September 8, 2021.

Digital Object Identifier 10.1109/ACCESS.2021.3107554

Metric Learning Based Convolutional Neural Network for Left-Right Brain Dominance Classification

ZHENG YOU LIM[1], KOK SWEE SIM[1], (Senior Member, IEEE), AND SHING CHIANG TAN[2]
[1]Faculty of Engineering and Technology, Multimedia University, Melaka 75450, Malaysia
[2]Faculty of Information Science and Technology, Multimedia University, Melaka 75450, Malaysia

Corresponding author: Kok Swee Sim (kssim@mmu.edu.my)

This work was supported in part by the Telekom Malaysia Research and Development Sdn. Bhd., Malaysia for the research project of Left and Right Brain Balancing Application with Electroencephalogram Biofeedback System under Grant MMUE/190088.

This work involved human subjects or animals in its research. Approval of all ethical and experimental procedures and protocols was granted by the Research Ethics Committee (REC) of Collaboration and Innovation Center (CIC) of Multimedia University Malaysia under Application No. EA0022020.

ABSTRACT The educational concepts upholding the theory of brain dominance have been developed for more than 30 years. Some academicians developed a series of the syllabus to exploit the brain capability of students by training their weaker hemisphere of the brain. Prior to training the weaker side of the brain with the developed syllabus, the brain dominance of the student shall be determined. All the current methods used to determine brain dominance are questionnaire-based assessments. There is a possibility that questionnaire biases could exist and lead to inaccurate results. In this research, we introduce a deep-learning method to classify brain dominance based on the electroencephalogram (EEG) signal that reflects the bio-information of the brain. In this paper, we employ a series of EEG signal processing techniques and a state-of-the-art deep learning neural network namely Metric Learning Based Convolutional Neural Network (MLBCNN) to determine brain dominance. We prove that the brain dominance theory is valid and it can be determined by applying machine learning from the EEG signals. We also present the results that show the MLBCNN system can give the best performance as compared to the other benchmark neural network models of which its classification accuracy is 97.44%. Hence, this proposed method can contribute to the education field by providing a system to discover students' brain dominance and keep track of their brain training progress. In this way, the potential and capability of their brain can be fully unleashed.

INDEX TERMS Brain dominance, electroencephalogram, deep learning, metric learning, convolutional neural network.

I. INTRODUCTION

In the year 1981, Roger Sperry was awarded the Nobel Prize for publishing his experimental finding which is known as the split-brain experiment [1]. His split-brain experiment was conducted from the year 1959 to the year 1968. The finding from his experiment is that brain can be separated into two hemispheres: the left brain and the right brain. The two hemispheres carry out different functions. The right brain recognizes words but cannot analyze and pronounce the word. The left brain can recognize and analyze language and speech. Hence, the right brain serves as a memory center and the left brain serves as a language center [1].

His research later inspires many research studies in brain lateralization where the outcomes show that the two hemispheres of the brain have different regions that are in-charged of doing specific neural tasks such as analytical thinking, memory, imagination, and so on [2]. These studies show that the left brain is specialized in doing the tasks requiring analysis, logical thinking, and language whereas the right brain is specialized in doing the tasks involving creativity, arts, emotion, and memory [3].

The majority of people have a dominant brain, either left- or right-brain dominant. This explains the reason why some people are good in mathematics and analysis but are weak in

The associate editor coordinating the review of this manuscript and approving it for publication was Muhammad Sharif.

creative thinking and arts; they are left-brain dominant [4]. In contrast, the right brain dominant people have a higher level of creativity and high attainment in music or art but are weak in mathematics and logical tasks [5].

Some studies show that when someone can achieve brain synchronization or brain balancing, he/she is able to unleash the potential of the brain and can perform rapid learning as well [6]. Brain synchronization or brain balancing indicates that both hemispheres of the brain are almost equally strong, and this can be achieved with proper training [7]. Hence, academicians such as Betty Edwards and Makoto Shicida [8] developed a series of brain training education syllabus to train up the weaker hemisphere of the brain. Throughout the years in which these academicians conducted their developed syllabus, most of their students are able to expand their brain capability and have made extraordinary achievements at a younger age [8].

Before undergoing the brain synchronization training, a concern is to figure out which side of a student's brain is dominant, whether he/she is left-brain dominant or right-brain dominant. The current methods employed to determine brain dominance are based on questionnaire methods such as the Stroop test, Hermann Brain Dominance Instrument, etc [9]. There is no biological information that can be referred to indicate the brain dominance of a person. The biological information can be retrieved from data that reflect brain activities. Currently. several technologies can be used to capture brain activities. Among these technologies, the EEG is the best choice as the EEG device is non-intrusive, handy, and affordable [10].

The EEG method measures the emitted electrical waves (also known as brainwaves) on the scalp by using conductive electrodes. The electrical waves are induced by the traveling of electrical signals throughout the billions of nerve cells [11] The EEG signal is an oscillating waveform where the amplitude and frequency of the waveform vary in time, depending on the activity state of the brain [12]. However, to the best of our knowledge, no research has yet been conducted to identify brain dominance by analyzing EEG signal using machine learning method.

Besides, raw EEG signal is complicated and it is difficult to directly reveal the major difference and features from the EEG waveform. Hence, in our approach, a deep neural network system is proposed to classify left or right brain dominance by referring to the recorded EEG waveform. The reasons for employing the deep neural network method are: firstly, the traditional handcrafted features such as fast Fourier transform (FFT), entropy, etc., are not good enough techniques to identify accurately a waveform of left-brain dominance from the right brain dominance, or vice versa [13]. Deep learning has the capability to determine the major features on its own to classify data [14]. Secondly, the EEG waveform of different individuals at the same brain dominance might be different. Thus, analyzing the brain dominance solely from the handcraft extracted features might not be accurate. As the deep neural network can be trained with numerous datasets, the classification results are generally regarded as more accurate as compared to the traditional analysis method [15].

Currently, numerous deep learning methods such as convolutional neural network (CNN), long short term memory (LSTM), recurrent neural network (RNN), gated recurrent unit (GRU) have been applied to solve problems related to data classification. These established deep learning techniques perform supervised learning. The training process of these deep neural networks involves the calculation of loss (or error) based on the differences between actual and predicted outputs, and back-propagation of the error from deep to shallower layers to adjust the parameters (weights and/or biases) by using optimizer algorithms. In this research, we develop a deep learning neural network method, namely Metric Learning Based Convolutional Neural Network (MLBCNN). In this MLBCNN, a conventional 3-layer CNN is employed and its training process incorporates a Metric Learning method to uplift the classification performance. In the conventional CNN training process, the real number values from the CNN output layer are used as the logit values of the Softmax function. The output logit values in real numbers are generated through CNN based on a single training dataset. All training data samples are independent of each other even though they are from the same class. The correlation among the data samples is not taken into the account as the training parameter. Hence, CNN requires a large amount of training data samples to achieve high accuracy in classification. In MLBCNN, the Metric Learning method is used to compute distance among embedding feature vectors in metric space. The computed distances are the logit values for the Softmax function. The normalized Softmax value calculated using logits computed from the Metric Learning is then applied for calculating the cross-entropy loss. Then, the computed loss is backpropagated to adjust the parameters of the CNN during the training session. In this metric learning, the correlation among the training data samples is taken into account as a training parameter. Metric Learning is capable of training an accurate CNN with a smaller number of training data samples. Besides, this Metric Learning method is effective in learning from a dataset that shows high data sparsity, where the data samples are from different classes but their embedding feature vectors are highly similar to each other and distributed sparsely in the metric space. In this research, the EEG waveform of both classes (left and right) are observed highly similar to each other and no salient features can be referred from raw data to distinguish between the two classes. Hence, the MLBCNN system is developed in this research to classify the left and right brain dominance based on the resting EEG of a person.

II. RELATED WORKS

A. HERMANN BRAIN DOMINANCE INSTRUMENT

Hermann Brain Dominance Instrument (HBDI) is an instrument based on a questionnaire developed by William Ned

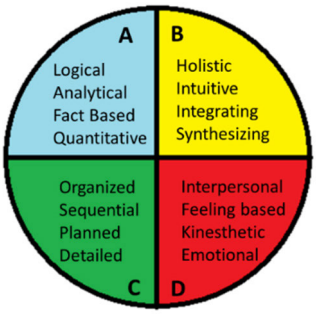

FIGURE 1. Four quadrant of whole brain model (Redrawn according to the description of whole brain® model in think Hermann-How it works) [16].

Hermann. It is used to evaluate the cognitive thinking preferences in people [16]. According to brain lateralization, each cognitive thinking style is dominantly based on either the left brain or right brain. Hence, this system is designed to measure the dominant hemisphere of the brain. It is a popular psychological assessment employed by numerous well-known companies such as IBM, Coca-Cola, etc [17] where this system is used to evaluate the thinking preferences and characteristics of the staff. According to the theory of HBDI, cognitive preferences are classified into four classes: analytical thinking, sequential thinking, interpersonal thinking, and imaginative thinking [18]. The brain dominance of a person is evaluated based on questionnaires in HBDI. The questions are specifically devised to calculate the scale of dominance for each of the four categories of cognitive preferences [19]. Figure 1 shows the HBDI four quadrant of cognitive thinking style, the illustration is redrawn according to the description of Whole Brain® Model in Think Hermann-How it works [16].

By using the HBDI assessment system, a person shall be informed of which cognitive thinking quadrant he is dominant. According to Figure 1, the person in either quadrant A or C is left-brain dominant, and the person in quadrant B or D is right-brain dominant. Quadrant A indicates that the person is dominant in analysis and logical thinking. Quadrant B indicates that the person has high capability in sequential thinking such as good in planning and scheduling. Quadrant C indicates that the person has high capability in interpersonal social, and communication. Quadrant D indicates that the person has high imaginative thinking and creativity [20]. Hence, this instrument is able to find out and show a person's brain is either left or right dominant.

However, the questionnaire-based assessment is a time-consuming process. The average time taken to complete each questionnaire is around 30 minutes. Another disadvantage of questionnaire assessment is that it could cause survey fatigue to the respondents after joining in repetitive assessments. This survey fatigue could happen because the questionnaire is too lengthy and the completion time is long. The survey could be incomplete or inaccurate when some respondents skip to answer difficult questions in detail or simply choose the answer without full consideration. Thus, a new method is proposed in this paper to determine left or right brain dominance with the biological information from the brain-waves (electroencephalogram) to overcome the weaknesses of questionnaire-based assessment.

B. LEFT-BRAIN VS. RIGHT-BRAIN HYPOTHESIS WITH RESTING STATE FUNCTIONAL CONNECTIVITY MAGNETIC RESONANCE IMAGING

Instead of using the electroencephalogram (EEG), the functional connectivity magnetic resonance imaging (rs-fcMRI) technique is another well-known method used to determine lateralization of the brain. By using this technique, Liu *et al.* [21] discovered that the language region is dominant in the left brain hemisphere, and the visual cortex is dominant in the right brain hemisphere. Tomasi and Volkow [22] found that there are short and long lateralized connections dominant around the lateral sulcus on the right brain hemisphere. On the other hand, there are fewer lateralized interconnections on the left brain hemisphere, which appeared at the medial areas of the occipital cortex. However, the lateralized interconnections may not be appropriate to justify the brain is left or right dominant. The structural asymmetry of the lateralized interconnections shall be further investigated to verify is it caused by the brain dominance of a person. Hence, Jared *et al.* [23] performed a research study to determine whether interconnectivity lateralization exhibits structural asymmetry. Besides, Jared *et al.* tried to determine whether or not brain dominance can be distinguished by referring to the rs-fcMRI results. Their results showed that the recognized left-dominant and right-dominant regions correlate to each other by having consistent lateralization interconnectivity. They discovered that the degree of lateralization is based on the brain regions which have a connection of interest. For example, Broca Area and Wernicke Area are language regions that are highly lateralized on the left hub. However, the results from rs-fcMRI were not consistent to indicate either a whole-brain phenotype of greater ''left-brained'' or a greater ''right-brained'' network strength across individuals. This finding showed the ineffectiveness of rs-fcMRI in identifying brain dominance. Hence, instead of rs-fcMRI, other techniques such as the EEG method could be useful to determine either left or right brain dominance of an individual.

C. EVALUATION OF LEFT AND RIGHT BRAIN DOMINANCE USING ELECTROENCEPHALOGRAM SIGNAL

Lim *et al.* [24] demonstrated the correlation between brain dominance with electroencephalogram signals. In order to determine the subject is left or right-brain dominant, HBDI was employed as a benchmark in their research. In this research work, they applied several signal processing techniques to remove noise from the raw EEG signal and preprocess the raw EEG signal to ease data analysis. They employed Continuous Wavelet Transform (CWT) method to generate frequency-based waveform and frequency band charts. These

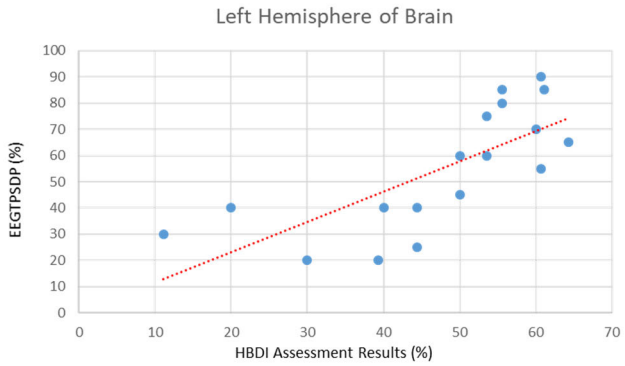

FIGURE 2. EEGTPSDP value (%) vs HBDI assessment result (%) for left brain [24].

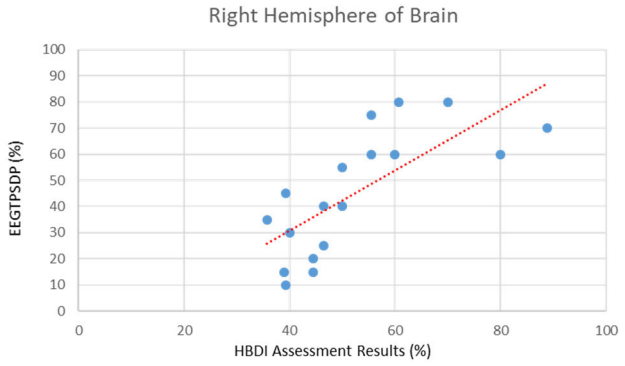

FIGURE 3. EEGTPSDP value (%) vs HBDI assessment result (%) for right brain [24].

pieces of information are used to analyze the brain activity between the left brain hemisphere and right brain hemisphere. Next, they implemented the EEG Topographical Power Spectral Density Percentage (EEGTPSDP) method which was used to compute correlation results between brain dominance and electroencephalogram. The EEGTPSDP value was calculated based on the PSD induced by the respective hemisphere. The results demonstrated that EEG signal has a high correlation with the dominant brain hemisphere based on the EEGTPSDP value. Figure 2 and Figure 3 illustrate the plot of EEGTPSDP value vs HBDI assessment results.

This research [24] showed that brain dominance in terms of EEGTPSDP has a high degree of correlation with the resting EEG signals. This presented a possibility that left/right brain dominance can be determined by learning patterns from the EEG signals. However, currently there is no classification method that can identify brain dominance based on the EEG signals in the resting state. Hence, we propose a method that utilizes a deep learning neural network to classify brain dominance based on the resting state EEG signals.

D. DEEP LEARNING FOR ELECTROENCEPHALOGRAM (EEG) SIGNAL CLASSIFICATION

Deep learning methods are commonly employed to discover and learn the features from the raw data by themselves. The terminology ''deep'' means that the artificial neural network architecture is composed of multiple hidden layers. The deep learning methods can automatically extract the high-level representative features that can be utilized to classify the input data into categories. Deep learning is useful in classifying the EEG signal because the features are difficult to be determined manually and the waveform patterns are different across different individuals [25].

To our best knowledge, no research work is found available in the literature to report the use of machine/deep learning methods for analyzing EEG signals for identifying brain dominance. However, there are several research works [26]–[30] that employed deep learning techniques to classify EEG signals for other purposes. In [26], Tang *et al.* employed a Deep Belief Network to categorize motor imagery for the left or right hand. They demonstrated the deep belief network achieved an average accuracy of up to 80% and the performance was 4% to 6% higher than a support vector machine.

In [27], Chen *et al.* employed the deep learning methods of convolutional neural network (CNN), multilayer perceptron (MLP), and support vector machine (SVM) to identify children with Attention deficit hyperactivity disorder (ADHD) based on EEG signals. From their findings, the CNN achieved classification accuracy up to 92.06% and outperform the MLP (84.75%) and SVM (84.17%).

In [28], Zheng *et al.* (2019) proposed a modified long short term memory (LSTM) neural network (named as long short term memory with bagging theory (LSTM-B)) to classify visualized images based on EEG signals. The concept of this framework was to predict visual scenes imagined from the brain based on the EEG signals. In this research, Zheng *et al.* demonstrated LSTM-B reached an accuracy up to 97.13% which was the highest as compared to the SVM method (82.7%), EEG-Net (88%), Pyramid Match Kernel (91.70%), recurrent neural network (84%) and bidirectional LSTM (97.10%).

Yuan *et al.* proposed a multilayer convolutional neural network (CNN) to detect epileptic seizures based on short-time Fourier transform (STFT) EEG signals [29]. They applied STFT to transform the raw EEG data from the time domain into the frequency domain. The frequency-domain EEG data were then used as the input to the CNN deep neural network. The proposed method could achieve the best accuracy up to 94.37% as compared to baseline models such as parallel SVM (79.46%) and probabilistic neural network (72.68%).

Farsi et al [30] performed the classification of an alcoholic person based on EEG signals. In this research, they employed two different machine learning methods and compared their performances. The first method employed principal component analysis (PCA) to extract the features and the extracted features were fed into the artificial neural network (ANN) for classification. The second method was an LSTM that learned information directly from the raw EEG signals. The results showed that the second method (LSTM) has a classification accuracy of 93% that was higher than 86% of the first method (PCA-ANN).

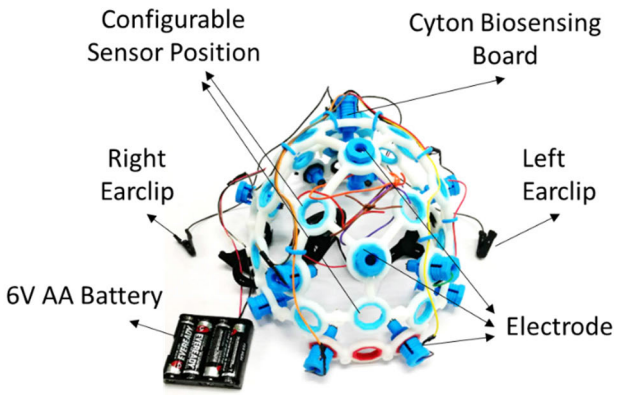

FIGURE 4. EEG device for EEG signal acquisition.

These research works [26]–[30] showed that deep learning neural networks have been applied to perform classification from the complicated raw EEG signals for the motor imaginary task, ADHD identification, visual scenes classification, epileptic seizure detection, and alcoholic person identification. To our best knowledge, we are the first group that utilizes deep learning neural networks to process EEG signals to identify an individual's brain dominance.

III. IMPLEMENTATION

This section explains the EEG device and the configuration employed in this research, subjects and EEG data collection procedure, dataset preprocessing techniques, and the implementation of Metric Learning Based Convolutional Neural Network (MLBCNN) for Classification.

A. EEG SIGNAL ACQUISITION DEVICE

In this research, we utilize OpenBCI Ultracortex Mark IV EEG Headset to record the EEG data from human subjects. Figure 4 shows the device employed in this research.

As shown in Figure 4, the wearable headset is made by using 3D printing technology. The 3D printed structure in white color is the frame of the headset. The headset consists of 35 node locations to customize the position of the sensors according to the research preferences. The configurable node locations are the holes on the headset that are printed with blue color plastic material. The headset is configurable into 8 channels or 16 channels of sensors. The sensor consists of dry conductive electrodes with an attached wire. The electrode holder is also 3D printed using blue color plastic material in a screw-like mechanism. The electrode holder is used to hold the dry conductive electrodes and it allows the sensor electrodes to mount onto the configurable node locations. Besides, there are two ear clips with attached wires on the left and right of the headset. They are used to clip on the earlobes and act as the signal ground. The wires of all the sensors are connected to a central unit which is known as the Cyton Biosensing Board that is located at the back of the headset. The Cyton Biosensing Board is powered by a 6V 4-AA battery power supply.

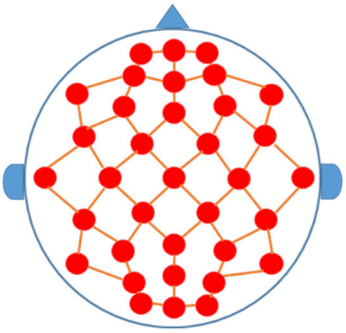

FIGURE 5. Customizable position of the sensors on OpenBCI Ultracortex Mark IV (Redrawn based on the image of Ultracortex Mark IV in OpenBCI shop) [31].

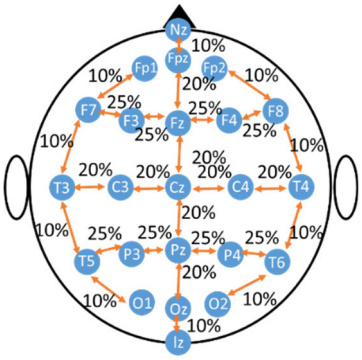

FIGURE 6. Customizable 35 sensor positions based on international 10/20 System [32].

The Cyton Biosensing Board is equipped with a wireless radio frequency chip. Hence, the board can communicate with the computer by using a radiofrequency USB dongle known as RFDuino. Besides, the Cyton Biosensing Board is also equipped with a Bluetooth Low Energy (BLE) module that allows the board to communicate with other devices via Bluetooth connection [31].

The 35 node locations of OpenBCI Ultracortex Mark IV EEG Headset are devised according to the International 10/20 system [32]. The '10' and '20' of 10/20 systems indicate the displacement percentage between the positions of each sensor. 10% indicates 10% of the total displacement from the forehead to the back of the head. Likewise, 20% means 20% of the total displacement from the forehead to the back of the head. In the 10/20 system, the position of the sensors is denoted by a letter followed by a number, for example, 'F2'. The letters indicate the region of the head: F, T, C, P and O. 'F' is the frontal lobe, 'T' is the temporal lobe, 'C' is the central part, 'P' is the parietal lobe, and O is the ''Occipital lobe''. Next, each letter is trailed by the letter 'z' or numbers. 'z' is the middle line, the odd number indicates the left hemisphere and the even number indicates the right hemisphere. Figure 5 indicates the customizable position of the sensor on Ultracortex Mark IV and Figure 6 shows an example of the International 10/20 system.

In this research, the headset is configured as an 8-channel device with 8 sensors at the following positions: FP1, FP2, F7, F8, F3, F4, T3, and T4. The position of electrodes is configured in a symmetrical manner on the left and right hemispheres. These sensors are positioned based on the lateralization function of the brain [33]. FP1 and FP2 are the active region of the brain for focusing and solving complex problems. F7 and F8 are the regions of memory. F3 and F4 are mainly functions for task management. Lastly, T3 and T4 are the language center and are major in reading and understanding. All the sensors are located in the frontal part of the head due to the rear part of the brain is mainly functioning for passive sensory information. As the left and right brain dominance theory is based on cognitive thinking, passive sensory information is not essential in this research.

B. SUBJECTS AND EEG DATA COLLECTION PROCEDURE

In this research, 60 sets of EEG data have been collected from 30 subjects. All of the subjects are male, age between 20 to 28 with no brain disease history and have an IQ score above 85 points. Before proceeding to the EEG data recording session, subjects are requested to complete the HBDI assessment to identify which brain is dominant. The HBDI assessment results will show the subjects are either left or right brain dominant.

In this research, the EEG signal is recorded when the subject is resting with open eyes. The EEG signal is not collected during the active state due to different activities might trigger different hemispheres of the brain. Hence, EEG signals during the resting state with eye-opening are the most neutral state and suitable to use for classifying the subject as either left or right dominant. In each process, two sets of resting-state EEG signals are obtained. The first set is recorded at the beginning of the process once the subject wore the headset properly with all the electrode sensors having good contact quality with the scalp. During the recording process, the subject is asked to relax his or her mind with open eyes. During this period, the EEG signal will be recorded for 2 minutes and it is labeled as Pre Resting-State EEG. Next, the subject is requested to perform some calculations and memory tests to keep the brain in an active state for around 5 minutes. No EEG signal will be recorded during this period. Lastly, the subject is asked to rest calmly again for 2 minutes, The EEG signal recorded during this period is labeled as Post Resting-State EEG. Then, these recorded resting-state EEG datasets are labeled according to the results obtained using the HBDI assessment. For example, the recorded EEG datasets will be labeled as ''left'' if the HBDI assessment result shows that the subject is left-brain dominant, and vice versa. Figure 7 shows the EEG datasets labeled with HBDI assessment results for training the proposed neural network.

C. COMPUTER SPECIFICATIONS

The hardware specifications of the computer employed in this research for training the deep learning neural network models are: Intel Core i7-9700K, 16GB random access memory (RAM), 500GB solid-state drive (SSD), and Nvidia RTX-2080TI graphics processing unit (GPU).

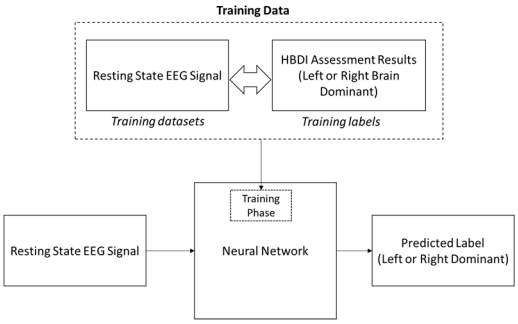

FIGURE 7. Recorded EEG datasets labeled with HBDI assessment results for training the proposed neural network.

D. EEG DATASET PREPROCESSING

The amplitudes of EEG electrical signal are low and this causes the raw EEG signal without amplification to be impractical for analysis. Thus, every EEG device is equipped with a digital amplifier circuit that amplifies the acquired signal. However, some noises caused by electrical line noise and other muscular activity will be amplified too. Thus, a series of signal preprocessing procedures is required to get rid of the unwanted artifacts from the acquired raw EEG signal.

Besides, due to hardware limitations, some data might be lost during wireless transmission. This causes the number of data samples to be incomplete. In our case, the sampling frequency of the EEG device is 250Hz, which means that 250 data per second. However, due to the data transmission loss, some of the cycles might not consist of the complete 250 samples per second. This will cause an unequal number of data samples per second.

The acquired 8-channel EEG data are saved as comma-separated value (CSV) files. Table 1 shows a few rows of the dataset in the CSV file of a sample. The first column is the label number of the sample in one second, the label number starts from 0 to 249 and repeats for another second. The data ''ch1'' to ''ch8'' are the values of the 8 channels. The data ''x'', ''y'', and ''z'' are the accelerometer value which is not utilized in our research. The last column is the timestamp for each obtained dataset. In Figure 8, a plot is constructed based on the values from the CSV file.

The value of raw EEG signal is ranged from -10000 to 70000, as shown in Figure 8. Hence, all EEG signals shall be normalized before processing them in the deep neural network. As mentioned that some data might be lost due to hardware limitation and wireless data transmission, an unequal number of samples per second in each dataset are not suitable for deep learning classification purposes. Hence, we implement a technique known as sample rebalancing to equalize the number of samples in each dataset. As the sampling frequency of the device is 250Hz, we set the minimum number

TABLE 1. Acquired EEG data in CSV format.

No	ch1	ch2	ch3	ch4	ch5	ch6	ch7	ch8	x	y	z	Timestamp
0	0	0	0	0	0	0	0	0	0.056	0.944	0.272	19:25:00.615
1	55028.85	4656.76	-20053.2	-20712.2	-19999.6	-20143.7	-385.14	-17094.3	0	0	0	19:25:00.630
2	55151.27	4650.62	-20057.6	-20713.5	-20001.6	-20147	-381.61	-17100.6	0	0	0	19:25:01.112
3	55255.28	4646.84	-20062.3	-20713.7	-20004.9	-20147.8	-383.69	-17106.3	0	0	0	19:25:01.112

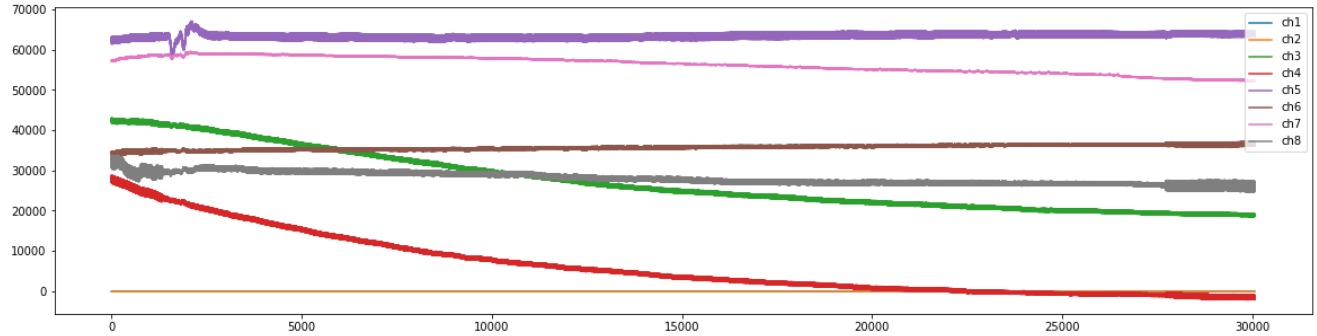

FIGURE 8. Plot of 8-channel EEG data in 2 minutes.

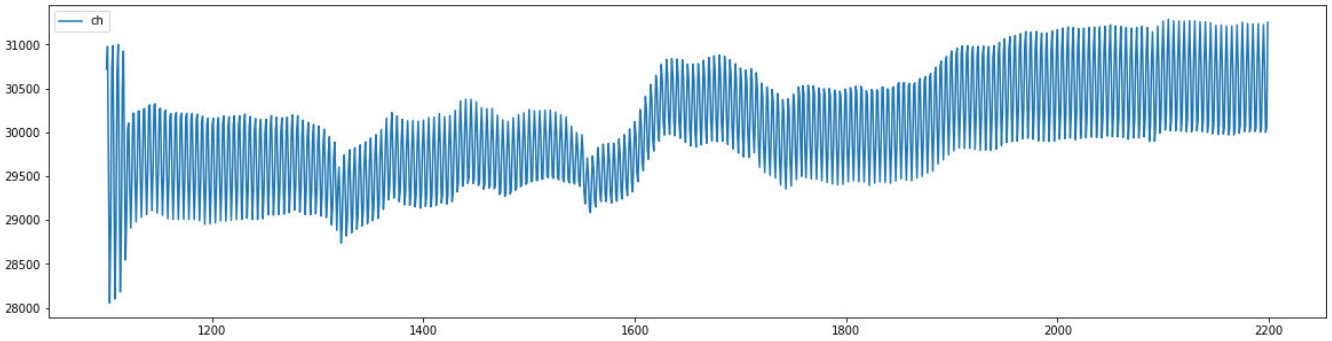

FIGURE 9. Plot of channel 8 EEG signal before spike removal.

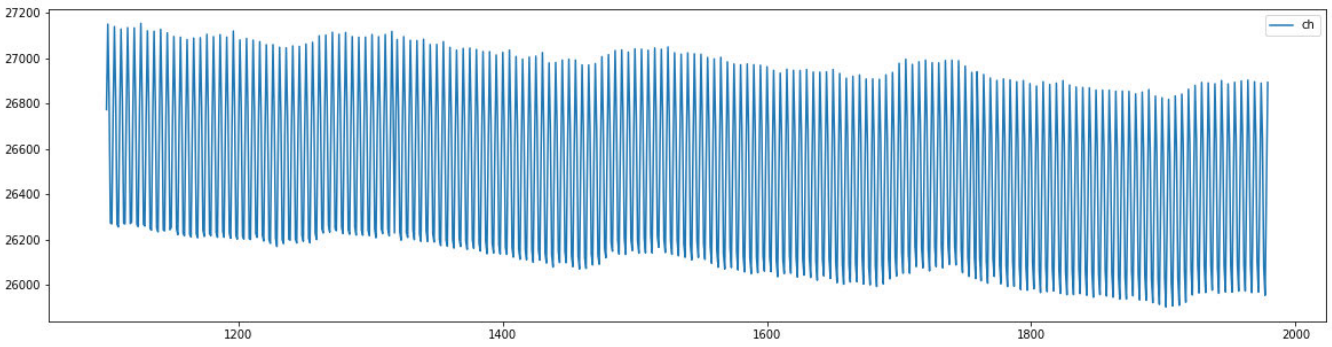

FIGURE 10. Plot of channel 8 EEG signal after spike removal.

of sample rows per dataset to 220 rows per second. In this technique, the datasets which have less than 220 sample rows are removed. The remaining datasets are truncated into 220 sample rows per second in order to obtain an equalized number of samples. Hence, each dataset has 220 (sample rows per second) $\times$ 8 (channels).

The muscular activity or eye blinking will cause a spikey noise in the acquired signal. This type of noise can be observed from channel 1 during the time of 1000 to 2500 or channel 8 during the time of 0 to 2000 in Figure 8. Figure 9 shows the zoomed-in view for channel 8 from 0 to 2000 of the time unit.

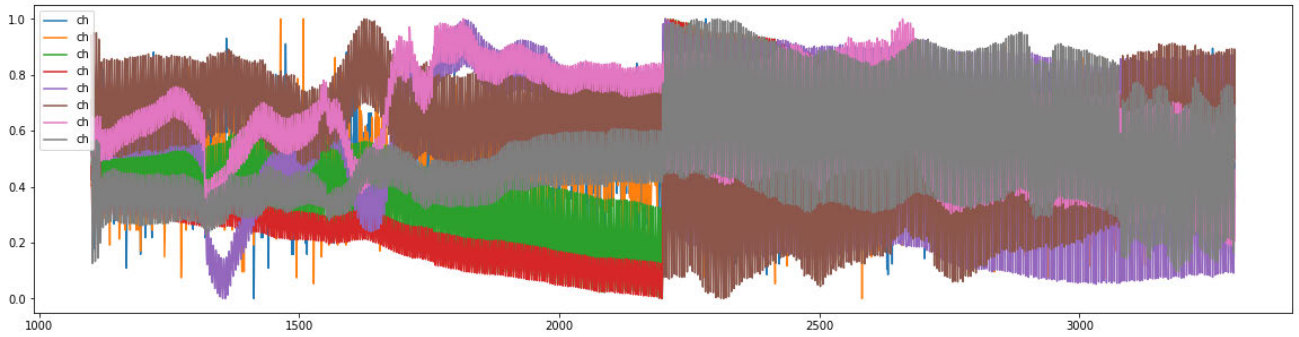

FIGURE 11. Plot of normalized EEG signals for 8 channels.

The spikes will cause a sudden shift of amplitude level in the waveform. Hence, the spike removal technique is constructed by defining the value of margin. The margin act as the corridor where the signals oscillate within the range of the margin. Hence, the waveform will be fitted in the corridor with the predefined margin level. The values above or below the predefined margin will be trimmed off. Figure 10 shows the example of the waveform after being applied with the spike removal technique.

The last technique applied for the EEG signal preprocessing is signal normalization. The raw EEG signals span a wide range between -10000 and 70000. In addition, the signals from the 8 channels might have different baseline voltage and fluctuate amplitudes. If these EEG signals are not normalized, they are not suitably used as input data to the deep neural network. Hence, a signal normalization technique is applied to the EEG signals to normalize them into values within a range between 0.0 to 1.0. Figure 11 shows the plot of the normalized EEG signal of the 8 channels.

In this research, 60 EEG datasets were collected from the subjects by following a data collection procedure explained in Section III(B). Each dataset has 120 samples (1 sample/second). Hence, there is a total number of 7,200 data samples employed in this research. In the experiment, 50 datasets (6000 data samples) are employed to train the neural network and 10 datasets (1200 data samples) are employed to test the trained neural network. The 50 datasets are further split into 80% for training dataset for training the neural network, and 20% for development (dev) sets, also known as validation data for examining the accuracy/loss of the training in each epoch of training for backpropagation purpose. Unlike the dev dataset, the testing datasets are the unseen data used to evaluate the fully trained neural network model. Figure 12 shows the distribution of datasets for neural network training.

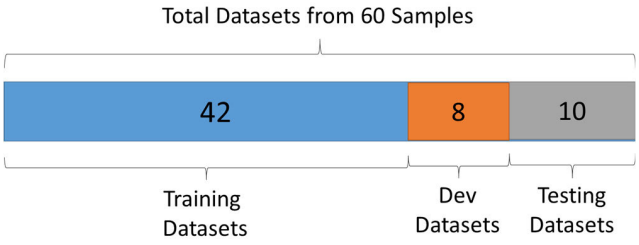

FIGURE 12. Distribution of datasets for neural network training.

E. METRIC LEARNING BASED CONVOLUTIONAL NEURAL NETWORK (MLBCNN) FOR CLASSIFICATION

In this research, the deep neural network model employed for classification is a convolutional neural network (CNN) with 3 convolutional layers. The conventional training process involves the calculation of error value based on predicted value and actual value using a cross-entropy loss function. Then, the error value will be backpropagated within the architecture of the neural network to adjust its parameters (weights or biases) using an optimizer algorithm. However, the training process of the proposed CNN in this research is modified based on the metric learning concept. The metric learning is applied in unsupervised learning. During the training process, metric learning will reduce the distance between the feature vectors with high similarity [34]. As a result, the feature vectors that have a high similarity to each other will be clustered together in the metric space. Hence, as inspired by the metric learning process, the training process for the implemented CNN in this research is modified with metric learning. The reason for modifying the training process using metric learning is because the EEG waveform of both left and right brain dominant are highly similar to each other. No salient features can be extracted to differentiate the EEG waveform of left-brain dominant and right-brain dominant. This cause high data sparsity where the feature embedding vectors of both classes are distributed sparsely and not clustering among the respective class in the metric space. Hence, this property causes increases the difficulty in classifying the EEG signal accurately.

1) CONVOLUTIONAL NEURAL NETWORK

A conventional 3-layered convolutional neural network (CNN) is constructed as the deep neural network for classification in this research. The reason for choosing CNN in

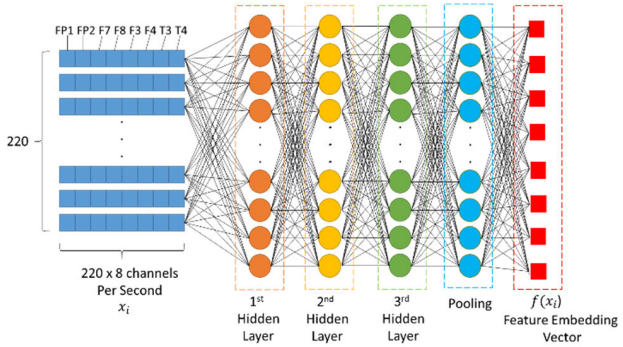

FIGURE 13. Convolutional neural network model architecture for encoding feature embedding vector from EEG data.

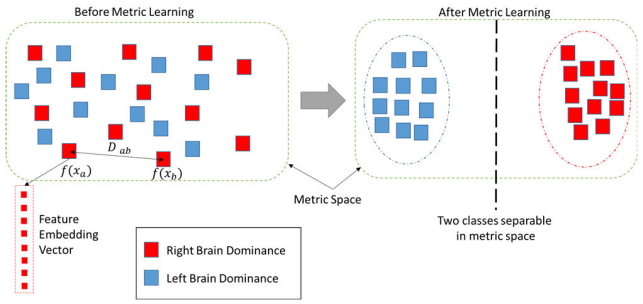

FIGURE 14. Concept of metric learning for left and right brain dominance classification.

this research is that CNN has a high capability of extracting important features and relationships from the 2-dimensional data array. Besides, the CNN also acts as a feature encoder to encode the raw EEG data into a feature embedding vector. These embedding feature vectors will be used in metric learning. Figure 13 shows the CNN model architecture employed in this research.

The input of the CNN autoencoder is the EEG data in a 2D matrix form with the dimension of 220 × 8, denoted as x_i. The CNN model is built by 3 hidden layers and a pooling layer. The first hidden layer is a 1D convolutional layer with 109 columns × 32 rows of nodes. In this 1st hidden layer, 32 filters with the kernel size of 3 × 3 are constructed.

Next, in the second hidden layer, it is another 1D convolutional layer with the shape of 54 columns × 64 rows of nodes. This convolutional layer is constructed with 64 filters with a kernel size of 3 × 3. The last hidden layer is also a 1D convolutional layer with the shape of 26 columns × 128 rows of nodes. It is constructed with 128 filters with a kernel size of 3 × 3. Then, the output of the 3rd hidden layer is linked to the pooling layer. This layer uses the averaging method to convert the output shape of 3rd hidden layer from 26 columns × 128 rows into 1 column × 128 rows. Finally, the output of the pooling layer is also further pooled into 8 nodes. And this final output with the size of 8 is known as the encoded feature embedding vector, denoted as $f(x_i)$.

2) METRIC LEARNING

At the beginning of the training process, every set of encoded feature embedding vectors are scattered randomly in the metric space. This is due to the EEG waveform for both left and right brain dominant are highly similar. Thus, the value of the feature vectors for both left and right classes are indistinguishable in the metric space. Hence, before training, all the feature embedding vectors are sparse. The vectors in the metric space are unable to be classified as all of them are scattered around. No simple function can be used to separate the two classes from the metric space. The concept of metric learning is illustrated in Figure 14.

As shown in Figure 14, the sets of feature embedding vectors represented in blue and red boxes are scattered around in the metric space. The red box represents the feature embedding vector for right-brain dominance EEG data, and the blue box represents the feature embedding vector for right-brain dominance. During the metric learning process, two pairs of feature embedding vectors will be selected. Each pair of the vectors consist of an anchor vector and another will be either a positive vector (if it is from the same class as the anchor vector) or a negative vector (if from a different class). During the selection process, the anchor vectors in both pairs must be from different classes. For example, if the anchor vector of the first pair is from the "Left" class, the anchor vector in the second pair must be from the "Right" class. In each pair of vectors, the anchor vector is selected based on the class label and the location in metric space. In the first pair, the vector with the class of "Left" shall be given the first priority of selection as the anchor vector when both vectors are from different classes. If both vectors are from the "Left" class, the one located at the leftmost in the metric space will be selected as the anchor vector. If both vectors are from the "Right" class, the one at the rightmost in the metric space will be selected as the anchor vector. For the second pair, the class of the anchor vector must be different from the class of the anchor vector in the first pair. If this criterion is not fulfilled, the second pair of vectors will be re-selected randomly. In the second pair, the vector with the class of "Right" shall be given the first priority of selection as the anchor vector when both vectors are from different classes. If both vectors are from the "Right" class, the one located at the rightmost in the metric space will be selected as the anchor vector. Then, the distances of the pair of feature embedding vectors will be computed, denoted as D_{ab}. The distances are computed between the positive/negative vector with the anchor vector within each pair and with the anchor vector of opposite pairs, denoted as D_{ab_1} and D_{ab_2}. The MLBCNN in this research is trained in 30 epochs with 100 batches of feature embedding vector pairs per epoch. A new selection of feature vector pairs is performed in each batch. In each iteration of the training process, the positive vector will move towards the anchor vector (line 6 in Algorithm 1). Hence, the distance between the anchor vector and the positive vector will become closer.

Algorithm 1 Algorithm for Metric Learning

Input: Feature Embedding Vector of Anchor Vector, $f(x_a)$ and Feature Embedding Vector of Data Vector, $f(x_b)$
Output: Updated Feature Embedding Vector of Data Vector, $f'(x_b)$

1: $epochs \leftarrow 30$
2: $temp \leftarrow 0.2$
3. **for** i=0 to $epochs$ **do**
4: Compute $D_{ab} \leftarrow ||f(x_a) - f(x_b)||^2$
5: **if** $f(x_b)$ is positive vector (same class with $f(x_a)$ **then**
6.: $f'(x_b) \leftarrow f(x_b) + (D_{ab} * temp)$
7: **else**
8: $f'(x_b) \leftarrow f(x_b) + (D_{ab}/temp)$
9: **end if**
10: **end for**
11: return $f'(x_b)$

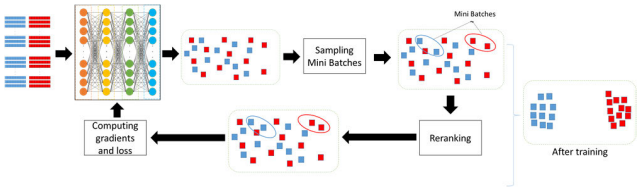

FIGURE 15. Metric learning based convolutional neural network for left and right brain dominance classification.

The process is vice versa for the negative vector (line 8 in Algorithm 1), where the negative vector will move further from the anchor vector. Hence, at the end of the training, the vectors of the same class will be clustered together. Hence, two classes are easily separable with a linear function. The algorithm of metric learning is shown in Algorithm 1. The detailed learning process of the MLBCNN is illustrated in Figure 15.

In the diagram illustrated in Figure 15, the EEG data are fed into the convolutional neural network to transform into feature embedding vectors. After transformed the data in metric space, mini-batches made up of pairs of vectors are randomly sampled. Each pair are either an anchor-positive or anchor-negative pair. Then, each batch will go through a re-ranking process. During the re-ranking process, the distance between the pair of vectors is calculated based on cosine similarity using (1).

$$D_{ab_i} = \frac{\sum_{j=1}^{8} A_j B_j}{\sqrt{\sum_{j=1}^{8} A_j^2}\sqrt{\sum_{j=1}^{8} B_j^2}}, \quad i = 1, 2 \tag{1}$$

where D_{ab} is the distance of anchor feature vector a and positive/negative feature vector b; A is the component in anchor feature vector a and B is the component in positive/negative feature vector b. j is from 1 to 8 due to each feature vector has the size of 8 for the 8 channels of EEG signal. When $i = 1$, the anchor vector, a is the anchor vector in the first pair. When $i = 2$, the anchor vector, a is the anchor vector in the second pair. Next, the logit value is computed based on D_{ab_i} using (2).

$$L_i = \begin{cases} \dfrac{D_{ab_i}}{\mu}, & \textit{if } a \textit{ and } b \textit{ are from the same class} \\ D_{ab_i} * \mu, & \textit{if } a \textit{ and } b \textit{ are from the different class} \end{cases} \tag{2}$$

where L_i is the computed logit value for $i = 1, 2$. The μ is the temperature coefficient value that is preset to 0.2. The μ is the hyperparameter in this neural network model.

Next, the logit values are substituted in a Softmax function for normalization. A softmax function is defined as (3).

$$f(x_i) = \frac{e^{x_i}}{\sum_{j=1}^{n} e^{x_j}} \tag{3}$$

where x_i is the input logit value for class i=1, 2. In this research, $n = 2$ as there are only two classes for classification. In the conventional method, the logit value is the real number value computed at the output node of the CNN for the correct class. The Softmax function is used to compute the probability among all classes in the range of [0,1]. For the Softmax function of MLBCNN, the logit values are computed using (2). By substituting the logit values from (2) into (3), the Softmax value is computed using (4).

$$f(L_i) = \frac{e^{L_i}}{e^{L_1} + e^{L_2}} \tag{4}$$

where $f(L_i)$ is computed Softmax value class $i = 1, 2$, L_1 is the logit value computed for the anchor vector in the first pair and L_2 is the logit value computed for the anchor vector in the second pair. Then, the computed Softmax value is used to calculate the cross-entropy loss using (5).

$$CE_i = -\sum_i t_i log(f(L_i)) \tag{5}$$

where L is the cross-entropy loss, t is the ground-truth value, i = 0, 1 for two classes.

$$\nabla = -\sum_i t_i \frac{\delta log(f(L))}{\delta o_i} \tag{6}$$

∇ is the computed gradient value, and o is the output value on the neuron. The gradients and loss values are then back-propagated to adjust the weights in the MLBCNN using the optimizer algorithm, namely Adaptive Moment Estimation (Adam) with a learning rate of 0.001. After 30 iterations of training, the weights in the MLBCNN are optimized in the way that all the feature embedding vectors from the same class will be clustered together and they are far away from clusters of another class in the metric space. Hence, the MLBCNN now is ready to perform classification.

After MLBCNN has been trained, its classification performance is evaluated in the testing phase. In this phase, the input EEG data will be first encoded into feature embedding vectors. Then, the input EEG data will be predicted as the nearest neighbor class based on the distance in metric space calculated using (1). The logit values will be then applied with the Softmax function in (3) to determine the confidence value of the predicted class.

IV. RESULTS AND DISCUSSION

The Metric Learning Based Convolutional Neural Network implemented in this research is evaluated in an ablation study. Besides, the MLBCNN also benchmarked with the other state-of-the-art deep learning techniques: CNN [35], Recurrent Neural Network (RNN) [36], Bidirectional RNN (Bi-RNN) [36], Long Short Term Memory (LSTM) [37], Bidirectional LSTM (Bi-LSTM) [37], Gated Recurrent Unit (GRU) [38], Bidirectional GRU (Bi-GRU) [38], ResNet [39], Inception-ResNet [40] and EfficientNet [41].

A. PERFORMANCE METRICS

As mentioned in Section III Figure 12, the 10 sets of testing data, which consist of 5 left-brain dominance and 5 right-brain dominance, are employed to measure the capability of the neural network. First, the metric used to measure the capability of the deep neural network is accuracy. Accuracy is the total number of correct predictions for left and right brain dominance over the total number of samples as in (7).

$$\textit{Accuracy}\ (\%) = \frac{\textit{Total Number of Correctly Predicted Samples}}{\textit{Total Number of Sample}} \times 100\% \tag{7}$$

Besides accuracy rate, precision rate and recall rate are other two common metrics employed to assess the capability of the neural network. Precision rate is the total number of correct predictions of a class over the total number of predictions of the respective class as in (8). The recall rate is defined as the total number of correct predictions of a class over the total number of all the samples belongs to the respective class as in (9). In addition, the neural network can be also assessed by another metric known as the F1 score. The F1 score can be calculated using (10).

$$\textit{Precision}\ (\%) = \frac{\dfrac{\textit{True Left}}{\textit{True Left}+\textit{False Left}+\dfrac{\textit{True Right}}{\textit{True Right}+\textit{False Right}}}}{2} \times 100\% \tag{8}$$

$$\textit{Recall}\ (\%) = \frac{\dfrac{\textit{True Left}}{\textit{True Left}+\textit{False Right}+\dfrac{\textit{True Right}}{\textit{True Right}+\textit{False Left}}}}{2} \times 100\% \tag{9}$$

$$\textit{F1 Score}\ (\%) = 2 * \frac{\textit{Precision} * \textit{Recall}}{\textit{Precision} + \textit{Recall}} \tag{10}$$

B. ABLATION STUDY

The proposed Metric Learning Based Convolutional Neural Network (MLBCNN, named as Model_3) method is a deep learning model that employs a convolutional neural network with 3 convolutional layers for feature embedding and metric learning as the classifier. Hence, in this research, an ablation study is performed to determine the performance contributed by the CNN and its convolutional layers. Three ablated models are defined in this research: (1) model with only metric learning and without CNN (Model_0), (2) MLBCNN of which the CNN consists of 1 convolutional layer (Model_1), (3) MLBCNN of which the CNN consists of 2 convolutional layers (Model_2).

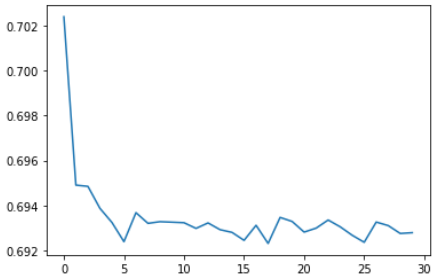

FIGURE 16. Training losses versus epochs for Model_0.

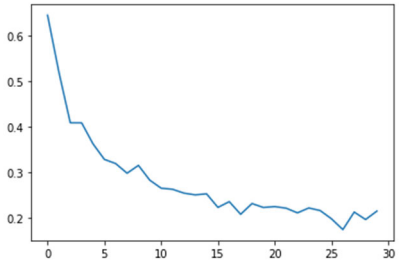

FIGURE 17. Training losses versus epochs for Model_1.

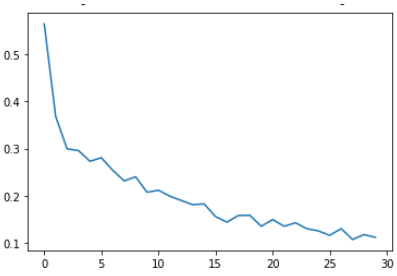

FIGURE 18. Training losses versus epochs for Model_2.

TABLE 2. Classification performances of ablated models.

Model	Accuracy (%)	Precision (%)	Recall (%)	F1 Score (%)
Model_0	60.56	60.26	60.26	60.26
Model_1	90.46	90.46	90.47	90.56
Model_2	93.43	93.49	93.51	93.50
Model_3	**97.44**	**97.44**	**97.44**	**97.44**

The training losses versus the number of epochs are illustrated from Figure 16 to Figure 19. The results show that Model_0 achieves the minimum loss rate of 0.692 within 5 epochs. Model_1 takes 26 epochs to achieve the minimum loss rate of 0.15. This shows a drastic improvement with the use of CNN as the feature embedding model. Next, Model_2 further reduces the loss rate to 0.1 in 27 epochs. Lastly, for the full MLBCNN model, Model_3 achieves the lowest error rate which is 0.02 in 22 epochs. This shows that the proposed full model has the best performance in terms of training loss rate versus the number of epochs.

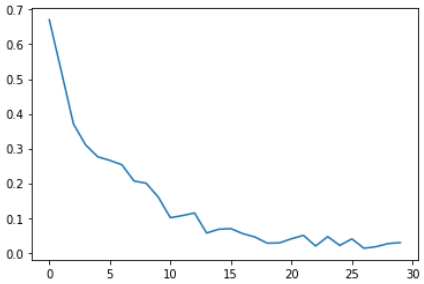

FIGURE 19. Training losses versus epochs for Model_3.

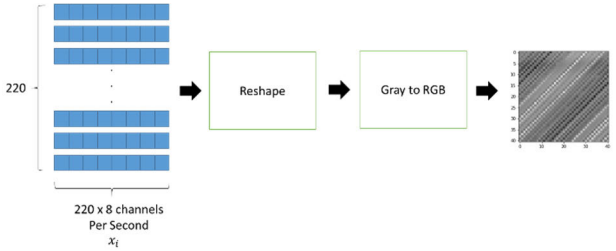

FIGURE 20. The process of EEG data transformation.

The classification performances are measured in terms of accuracy, precision, recall, and F1 score. According to the results in Table 2, Model_0 has the lowest accuracy, precision, recall, and F1 score of around 60%. For Model_1, by using the CNN with 1 convolution layer as the feature embedding encoder before the metric learning classifier, all the performance metrics drastically improves to around 90%. For Model_2, by using the CNN of 2 convolution layers, the performance metrics improve by 3%. Lastly, the Model_3 with a CNN of 3 convolution layers achieves the highest performance in terms of accuracy, precision, recall, and F1 score of 97.44%. The ablation study shows the CNN that is deployed as the feature embedding encoder plays an important role in the entire deep learning model. The CNN encoder uplifts the classification performances up to 30% as compared to the metric learning classifier without CNN (Model_0). The second and third convolution layers of the CNN (i.e., Model_1 and Model_2) could further improve classification performances by 3% to 4%.

C. DEEP LEARNING NEURAL NETWORK FOR BENCHMARKING

1) CONVOLUTIONAL NEURAL NETWORK (CNN)

The CNN model employed for benchmarking in this research are: conventional CNN [35], ResNet [39], Inception-ResNet [40] and EfficientNet [41]. The conventional CNN is made up of two 1-dimensional convolution layers, two batch normalization layers, and two pooling layers. The model is illustrated in Figure 21(a).

The input is exactly the same as the model illustrated in Figure 13 in Section III, with the size of 220 rows $\times$ 8 columns. The input layer is connected to the first 1D convolutional layer. The convolutional layer applies numerous kinds of filter masks to the input data and produces the masked results [35]. The first convolutional layer involves 32 filters with a kernel size of 3 $\times$ 3. The masked results are then connected to the batch normalization layer. This layer will normalize the value of the masked results. Then the normalized results are connected to a pooling layer. This layer will scale down the shape size of the data using the compression technique. The first pooling layer has a pooling size of 5, which means 5 nodes will be compressed into 1 node. The resultant nodes are then connected to the second cascaded layers of a 1D convolutional layer with 64 filters and a mask size of 1 $\times$ 3, a batch normalization layer, and a pooling layer with a pooling size of 3. Finally, the network is connected to the output layer with 2 nodes which indicates the 2 classes: left and right (brain dominance).

The other three CNN-based state-of-the-art models, namely ResNet [39], Inception-ResNet [40], and EfficientNet [41] are employed (with default settings) in a benchmark study in this research for performance comparison. However, as these neural networks are designed for processing colored images, an additional transformation process is required to convert the EEG data from 2D into 3D as the input data. Figure 20 illustrates the process of EEG data transformation.

The EEG data with the dimension of 220 $\times$ 8 is first passed to the reshape process. During this process, the 2D data is reshaped to meet the desired input size of a CNN model. The desired size of ResNet is 32 $\times$ 32, Inception-Resnet is 299 $\times$ 299 and EfficientNet is 224 $\times$ 224. In this process, the data will be truncated if the desired input size is smaller than the original size, where each redundant element is filled up with a value '0' to achieve the desired size. Then, the 2D array with the desired size is converted into a colored image (3D) using a gray to red green blue (Gray to RGB) converter that is available in an open-sourced image processing library, OpenCV. Hence, the resultant 3D array can be used as the input data to the three state-of-the-art models for performance assessments.

2) RECURRENT NEURAL NETWORK (RNN) AND BIDIRECTIONAL RNN (BI-RNN)

Unlike CNN that is known as a feedforward model, a recurrent neural network (RNN) is a deep learning model that will pass the output information to the neighbor cells in the same hidden layer [36]. An RNN cell is illustrated in Figure 21(b).

In Figure 21(b), it shows that the input vector, x_t and hidden layer vector of the previous cell (if exist, value is zero if not exist), h_{t-1} are the input for the RNN cell. The RNN cell consists of an activation function of the hyperbolic tangent (tanh) and produces output, y_t and hidden layer vector, h_t for the next cell. The RNN model implemented for the benchmark [36] is shown in Figure 21(e). The input is connected to an RNN layer with 32 cells. The RNN layer is later connected with a dense of neural network layer of 32 cells. Then, the dense layer is connected to the output layer with 2 cells.

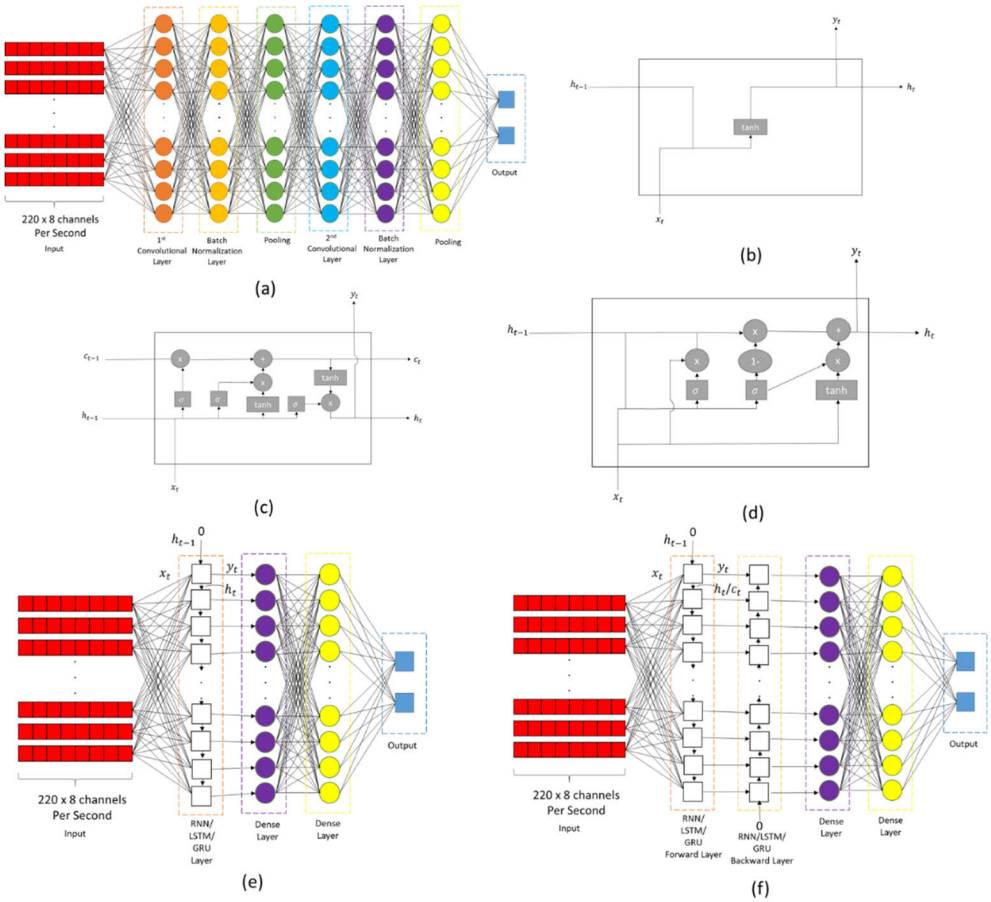

FIGURE 21. Deep neural network for benchmarking.

For bidirectional RNN (Bi-RNN), the neural network consists of one more layer namely the backward layer, where the hidden layer vector, h_t is fed to the next cell in the opposed direction of the previous RNN layer namely the forward layer. The forward layer and backward layer have the same number of cells. Each cell in the forward layer is linked to the respective cell in the backward layer. Figure 21(f) illustrates the bidirectional RNN neural network layer for benchmarking [36].

3) LONG SHORT TERM MEMORY (LSTM) AND BIDIRECTIONAL LSTM (BI-LSTM)

Long short term memory (LSTM) [37] is a modified neural network based on RNN. LSTM is slightly different from RNN, wherein the calculation within the cell of LSTM involves more activation functions and mathematical operations. Nonetheless, it has one more hidden layer vector which is c. Besides the activation function of the hyperbolic tangent (tanh), the cell also consists of another activation function of sigma, σ. The advantage of LSTM over RNN is the capability to preserve the information for a longer period of time.

The LSTM and Bi-LSTM neural network models [37] for benchmarking are illustrated in Figures 21(e) and 21(f).

4) GATED RECURRENT UNIT (GRU) AND BIDIRECTIONAL GRU (BI-GRU)

Gated recurrent unit [38] is also another deep neural network modified based on RNN. The activation function consists of a hyperbolic tangent (tanh) and sigma activation function, σ in the GRU cell. The advantage of GRU over LSTM is that it requires less memory space, shorter training, and execution time.

The GRU and Bi-GRU neural network models [38] are illustrated in Figures 21(e) and 21(f).

D. DEEP LEARNING MODELS PERFORMANCE ASSESSMENT

The performance of MLBCNN is benchmarked against with 7 deep learning models implemented in Section IV(C): CNN [35], Recurrent Neural Network (RNN) [36], Bidirectional RNN (Bi-RNN) [36], Long Short Term Memory (LSTM) [37], Bidirectional LSTM (Bi-LSTM) [37], Gated Recurrent Unit (GRU) [38], Bidirectional GRU (Bi-GRU) [38]. MLBCNN is also benchmarked against the 3 state-of-the-art models mentioned in Section II: ResNet [39], Inception-ResNet [40] and EfficientNet [41]. These three state-of-the-art models are employed with the

TABLE 3. Summary of deep neural network model.

Model	# of layers	Training time (s)	Applications
CNN [35]	6	30	Signal, Image Classification
RNN [36]	3	60	Time Series Signal Prediction
Bi-RNN [36]	4	90	Time Series Signal Prediction
LSTM [37]	3	246	Time Series Signal Prediction
Bi-LSTM [37]	4	365	Time Series Signal Prediction
GRU [38]	3	210	Time Series Signal Prediction
Bi-GRU [38]	4	274	Time Series Signal Prediction
ResNet152 V2 [39]	152	37,056	Image Classification
Inception-ResNet V2 [40]	164	34,918	Image Classification
EfficientNet-B7 [41]	813	644	, Image Classification
MLBCNN	**4**	**115**	**, Time Series Data Classification, Signal Classification**

TABLE 4. Performance of deep neural network model.

Model	Accuracy (%)	Precision (%)	Recall (%)	F1 Score (%)
CNN [35]	90	90.4	90	90.2
RNN [36]	54.5	71.6	54.5	60.2
Bi-RNN [36]	57	63.7	57	60.2
LSTM [37]	57	57	57	57
Bi-LSTM [37]	44.5	37.4	44.5	40.6
GRU [38]	79	82.3	79	80.8
Bi-GRU [38]	73	81.3	73	79.4
ResNet152 V2 [39]	88.66	88.66	88.68	88.66
Inception-ResNet V2 [40]	80.67	80.67	86.06	83.26
EfficientNet-B7 [41]	89.69	89.69	89.73	89.70
MLBCNN	**97.44**	**97.44**	**97.44**	**97.44**

default settings as in [39], [40], and [41]. The summary of the deep learning neural networks including the number of hidden layers, total training time for 30 epochs, and general application of the neural networks are tabulated in TABLE 3. The classification performances in terms of accuracy, precision, recall rate, and F1 score are tabulated in TABLE 4.

In TABLE 3, the results show that RNN, LSTM, and GRU have the lowest number of hidden layers. MLBCNN as well as Bi-RNN, Bi-LSTM, and Bi-GRU have the second-lowest number of hidden layers, which is 4. Other state-of-the-art CNN models such as ResNet, Inception-ResNet, and EfficientNet have a relatively very high number of hidden layers. CNNs are generally applied for signal classification and image classification. The general application of RNN, Bi-RNN, LSTM, Bi-LSTM, GRU, and Bi-GRU is time-series signal prediction. They are employed in this benchmark study because the EEG signal is time-series data. The state-of-the-art CNN models such as ResNet, Inception-ResNet, and EfficientNet are used in a benchmark study to compare the performance of the MLBCNN; these CNNs are mostly applied in image classification. The MLBCNN implemented in this research is applied for EEG signal classification. In terms of the training time, the results show the conventional CNN model requires the shortest training time (30 seconds), and this is followed by RNN (60 seconds) and Bi-RNN (90 seconds). The proposed method MLBCNN requires 115 seconds, which is the fourth-lowest training time. However, in TABLE 4, it shows that MLBCNN outperforms CNN, RNN, and Bi-RNN in terms of accuracy, precision, recall rate, and F1 Score. ResNet152 V2, Inception-ResNet V2, and EfficientNet-B7 consume very long training time especially the ResNet (∼10.29 hours) and Inception-Resnet (∼9.69 hours). Hence, the proposed MLBCNN outperforms the three state-of-the-art models in terms of much shorter training time and higher classification performances. The MLBCNN implemented in this research has achieved the best classification performance in terms of accuracy, precision, recall, and F1 of which the scores are 97.44%. These results show that MLBCNN could be trained efficiently to achieve very high efficacy when compared with other deep neural network models in classifying brain dominance from EEG signals.

V. CONCLUSION

In this research, several EEG data processing techniques have been developed to preprocess the input EEG signal. We also developed a deep learning neural network namely metric learning based convolutional neural network (MLBCNN) to determine brain dominance using preprocessed EEG signals. The results from the experimental study in this research show that the deep learning neural network models are capable of learning micro features from the EEG signals that are useful to distinguish EEG signals from left and right brain dominance. The proposed MLBCNN could achieve classification performances up to 97.44% in terms of accuracy, recall, precision, and F1 score. The MLBCNN has outperformed all the other state-of-art deep neural network models in a benchmark study.

This research shows an evidence that brain dominance can be determined after learning features from EEG signals by a deep learning approach. Hence, this research contributes to the education field in the future where the teachers can

determine the brain dominance of students and arrange suitable learning syllabus for the respective students. In this way, the student's brain capability and potential can be fully unleashed.

ACKNOWLEDGMENT

The author would also like to thank the subjects who are involved in the data collection for this research.

REFERENCES

[1] L. Dina. (Jun. 27, 2017). *Roger Sperry's Split Brain Experiments*. Embryo Project Encyclopedia. Accessed: Feb. 18, 2021. [Online]. Available: https://embryo.asu.edu/pages/roger-sperrys-split-brain-experiments-1959-1968

[2] O. Güntürkün, F. Ströckens, and S. Ocklenburg, "Brain lateralization: A comparative perspective," *Physiol. Rev.*, vol. 100, no. 3, pp. 1019–1063, Jul. 2020.

[3] M. Oflaz, "The effect of right and left brain dominance in language learning," *Procedia Social Behav. Sci.*, vol. 15, pp. 1507–1513, 2011.

[4] M. C. Corballis, "Left brain, right brain: Facts and fantasies," *PLoS Biol.*, vol. 12, no. 1, pp. 1–6, 2014.

[5] S. A. Ali and S. Raza, "A study of right and left brain dominant students at IB&M with respect to their gender, age and educational background," *Int. J. Adv. in Sci. Res.*, vol. 3, no. 9, pp. 115–120, 2017.

[6] A. Trafton. (Jun. 12, 2014). *Synchronized Brain Waves Enable Rapid Learning*. MIT News. Accessed: Feb. 18, 2021. [Online]. Available: https://news.mit.edu/2014/synchronized-brain-waves-enable-rapid-learning-0612

[7] M. Shaughnessy and C. Kleyn-kennedy, "An interview with Betty Edwards," *Int. J. Academic Res. Educ.*, vol. 2, no. 1, pp. 51–57, 2016.

[8] C. Choi. (May 20, 2013). *Popularity of 'Shichida' Education Bewilders Experts*. South China Morning Post. Accessed: Feb. 18, 2021. [Online]. Available: https://www.scmp.com/news/hong-kong/article/1241402/popularity-shichida-education-bewilders-experts

[9] H. Ashraf, T. Branch, and M. T. Yazdi, "Brain dominance quadrants and reflective teaching among ELT teachers: A relationship study," *Int. J. English Linguistics*, vol. 7, no. 2, pp. 63–72, 2017.

[10] K. S. Sim, Z. Y. Lim, and T. K. Kho, "Brainwave controlled electrical wheelchair," in *Proc. Int. Conf. Automat. Sci.*, vol. 1, 2016, pp. 10–15.

[11] K. S. Sim, Z. Y. Lim, and T. K. Kho, "EEG Controlled Wheelchair," in *Proc. MATEC Web Conf.*, vol. 51, 2016, pp. 18–25.

[12] K. S. Sim, Z. Y. Lim, and S. Fawaz, "Development of dementia neurofeedback system using EEG brainwave signals," *Int. J. Signal Process. Syst.*, vol. 7, no. 4, pp. 113–117, Dec. 2019.

[13] S. Fawaz, K. S. Sim, and S. C. Tan, "Encoding rich frequencies for classification of stroke patients EEG signals," *IEEE Access*, vol. 8, pp. 135811–135820, 2020.

[14] M. Elsayed, K. S. Sim, and S. C. Tan, "A novel approach to objectively quantify the subjective perception of pain through electroencephalogram signal analysis," *IEEE Access*, vol. 8, pp. 199920–199930, 2020.

[15] S. S. Alahmari, D. B. Goldgof, P. R. Mouton, and L. O. Hall, "Challenges for the repeatability of deep learning models," *IEEE Access*, vol. 8, pp. 211860–211868, 2020.

[16] *Herrmann's Core Idea: Whole Brain? Thinking*. Think Hermann. Accessed: Feb. 18, 2021. [Online]. Available: https://www.thinkherrmann.com/how-it-works/

[17] A. Belousova and V. Pishchik, "Technique of thinking style evaluating," *Int. J. Cognit. Res. Sci., Eng. Educ.*, vol. 3, no. 2, pp. 1–8, Dec. 2015.

[18] M. Sadeghi, H. R. Kolvir, A. Atadokht, and H. Akbari. (Oct. 30, 2020). *The Effectiveness of Mental Simulation Training on Educational Performance and Creativity of the Architecture Students in Therapeutic Spaces Design*. Research Square. Accessed: Feb. 18, 2021. [Online]. Available: https://europepmc.org/article/ppr/ppr232469

[19] H. M. Abdulkhaliq and A. A. I. Al-Halawachy, "Thinking styles: A theoretical account," *Academic J. Nawroz Univ.*, vol. 8, no. 4, pp. 339–346, 2019.

[20] A. K. A. Bawaneh, A. G. K. Abdullah, S. Saleh, and K. Y. Yin, "Jordanian students' thinking styles based on Herrmann whole brain model," *Int. J. Hum. Social Sci.*, vol. 1, no. 9, pp. 89–97, 2011.

[21] H. Liu, S. M. Stufflebeam, J. Sepulcre, T. Hedden, and R. L. Buckner, "Evidence from intrinsic activity that asymmetry of the human brain is controlled by multiple factors," *Proc. Nat. Acad. Sci. USA*, vol. 106, no. 48, pp. 20499–20503, Dec. 2009.

[22] D. Tomasi and N. D. Volkow, "Laterality patterns of brain functional connectivity: Gender effects," *Cerebral Cortex*, vol. 22, no. 6, pp. 1455–1462, Jun. 2012.

[23] A. N. Jared, B. A. Zielinski, M. A. Ferguson, J. E. Lainhart, and J. S. Anderson, "An evaluation of the left-brain vs. right-brain hypothesis with resting state functional connectivity magnetic resonance imaging," *PLoS ONE*, vol. 8, no. 8, pp. 1–11, 2013.

[24] Z. Y. Lim, K. S. Sim, and S. C. Tan, "An evaluation of left and right brain dominance using electroencephalogram signal," *Eng. Lett.*, vol. 28, no. 4, pp. 1358–1367, 2020.

[25] M. Mahmud, M. S. Kaiser, A. Hussain, and S. Vassanelli, "Applications of deep learning and reinforcement learning to biological data," *IEEE Trans. Neural Netw. Learn. Syst.*, vol. 29, no. 6, pp. 2063–2079, Jun. 2018.

[26] X. Tang, J. L. Zhou, N. Zhang, and Q. Liu, "Recognition of motor imagery EEG based on deep belief network," *Inf. Control*, vol. 44, no. 6, pp. 717–721, 2015.

[27] H. Chen, Y. Song, and X. Li, "A deep learning framework for identifying children with ADHD using an EEG-based brain network," *Neurocomputing*, vol. 356, pp. 83–96, Sep. 2019.

[28] X. Zheng, W. Chen, Y. You, Y. Jiang, M. Li, and T. Zhang, "Ensemble deep learning for automated visual classification using EEG signals," *Pattern Recognit.*, vol. 102, pp. 3–34, Jun. 2019.

[29] Y. Yuan, G. Xun, K. Jia, and A. Zhang, "A multi-view deep learning framework for EEG seizure detection," *IEEE J. Biomed. Health Inform.*, vol. 23, no. 1, pp. 83–94, Jan. 2019.

[30] L. Farsi, S. Siuly, E. Kabir, and H. Wang, "Classification of alcoholic EEG signals using a deep learning method," *IEEE Sensors J.*, vol. 21, no. 3, pp. 3552–3560, Feb. 2021.

[31] *Ultracortex Mark IV EEG Headset*. OpenBCI Online Store. Accessed: Feb. 18, 2021. [Online]. Available: https://shop.openbci.com/products/ultracortex-mark-iv

[32] E. Niedermeyer and F. L. da Silva, *Electroencephalography: Basic Principles, Clinical Applications, and Related Fields*. Oxford, U.K.: Oxford Univ. Press, 2004, p. 140.

[33] *Anatomy of the Brain*. Mayo Clinic. Accessed: Feb. 18, 2021. [Online]. Available: https://www.mayfieldclinic.com/pe-anatbrain.htm

[34] Y. Li, S. Kan, and Z. He, "Unsupervised deep metric learning with transformed attention consistency and contrastive clustering loss," in *Computer Vision* (Lecture Notes in Computer Science), vol. 12356. 2020, pp. 141–157.

[35] R. Xin, J. Zhang, and Y. Shao, "Complex network classification with convolutional neural network," *Tsinghua Sci. Technol.*, vol. 25, no. 4, pp. 447–457, Aug. 2020.

[36] W. Zhang, C. Li, T. Huang, and X. He, "Synchronization of memristor-based coupling recurrent neural networks with time-varying delays and impulses," *IEEE Trans. Neural Netw. Learn. Syst.*, vol. 26, no. 12, pp. 3308–3313, Dec. 2015.

[37] M. A. I. Sunny, M. M. S. Maswood, and A. G. Alharbi, "Deep learning-based stock price prediction using LSTM and bi-directional LSTM model," in *Proc. 2nd Novel Intell. Lead. Emerg. Sci. Conf. (NILES)*, Giza, Egypt, 2020, pp. 87–92.

[38] Y. Hao, Y. Sheng, and J. Wang, "Variant gated recurrent units with encoders to preprocess packets for payload-aware intrusion detection," *IEEE Access*, vol. 7, pp. 49985–49998, 2019.

[39] K. He, X. Zhang, S. Ren, and J. Sun, "Deep residual learning for image recognition," in *Proc. IEEE Conf. Comput. Vis. Pattern Recognit. (CVPR)*, Jun. 2016, pp. 770–778.

[40] C. Szegedy, S. Ioffe, V. Vanhoucke, and A. A. Alemi, "Inception-v4, inception-ResNet and the impact of residual connections on learning," in *Proc. 31st AAAI Conf. Artif. Intell.*, 2017, pp. 4278–4284.

[41] M. Tan and Q. V. Le, "EfficientNet: Rethinking model scaling for convolutional neural networks," in *Proc. Int. Conf. Mach. Learn.*, 2019, pp. 6105–6114.

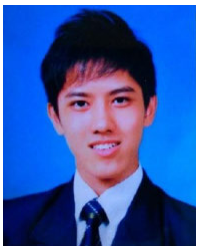

ZHENG YOU LIM received the Bachelor of Engineering degree (Hons.) electronics majoring in robotics and automation and the Master of Engineering Science (M.Eng.Sc.) degree from Multimedia University, Malaysia, in 2016 and 2019, respectively, where he is currently pursuing the Ph.D. degree in engineering. His research interests include robotics, automation, image processing, artificial intelligence, and electroencephalogram. He received the President Award upon his graduation of bachelor's degree, in 2016. He also received the Merit Winner in International APICTA Awards 2016 and Champion in WSIS Award 2018.

KOK SWEE SIM (Senior Member, IEEE) is currently a Professor with Multimedia University, Bukit Beruang, Melaka, Malaysia. He is also working closely with various local and overseas institutions and hospitals. He has filed 18 patents and more than 70 copyrights. He was a recipient of the Japan Society for the Promotion of Science (JSPS) Fellowship, Japan, in 2018. He has received many international and national awards, such as the Academic Science Malaysia (ASM) as Top Research Scientists Malaysia (TRSM), the Korean Innovation and Special Awards, in 2013, 2014, and 2015, the 2005, 2006, and 2011 World Conference in Applied Computing (USA), and the 2008 IEEE Conference at U.K. For national level achievements, he received the Gold Medal Award in the Invention, Innovative Technology Exhibition (ITEX) 2008, 2009, 2010, 2013, and 2014, the Bio Malaysia Award 2009 and 2010, the Malaysia Technology Expo 2011, AIK2011, AIK2012, and the APICTA Gold Medal Award 2014 and 2015. He received the MMU Best Staff Award, in 2009, 2010, and 2015. He received awards for the TM Kristal Award and two International Championships of World Summit on the Information Society (WSIS) Prizes in the category ICT applications, such as E-science, during the event held in conjunction with WSIS 2016, Geneva, Switzerland, in 2016. These awards were in the areas of biomedical Engineering (breast cancer detection and brain for early infarct detection). He received the WSIS International Championship Awards, in 2017, 2018, 2019, 2020, and 2021. He has received more than 80 awards which can be found in his website.

SHING CHIANG TAN received the B.Tech.(Hons.) and M.Sc. (Eng.) degrees from the Universiti Sains Malaysia, Malaysia, in 1999 and 2002, respectively, and the Ph.D. degree from Multimedia University, Malacca, Malaysia, in 2008. He is currently an Associate Professor with the Faculty of Information Science and Technology, Multimedia University. His current research interests include computational intelligence (artificial neural networks, evolutionary algorithms, fuzzy logic, and decision trees), and their applications, data classification, condition monitoring, fault detection and diagnosis, and biomedical disease classification. He was a recipient of the Matsumae International Foundation Fellowship, Japan, in 2010.